

Supplementary Information for:

Hyoliths with pedicles constrain the origin of the
brachiopod body plan

Haijing Sun, Martin R. Smith, Han Zeng, Fangchen Zhao, Guoxiang Li and Maoyan Zhu

2018-06-19

Contents

Supplementary Text	3
1 Phylogenetic dataset	4
2 Fitch parsimony	6
2.1 Results	7
3 Bayesian analysis	13
3.1 Parameter estimates	14
3.2 Results	14
4 Corrected parsimony	16
4.1 Search parameters	16
4.2 Analysis	16
4.3 Results	17
5 Character reconstructions	25
6 Taxonomic implications	27
Supplementary Figures	29
Supplementary Table	33
Bibliography	34

Supplementary Text

This document contains supplementary material to Sun et al. (2018). It is best viewed in HTML format at ms609.github.io/hyoliths.

It describes the morphological dataset and the results of tree searches using Fitch parsimony and a Bayesian method: approaches that are subject to errors resulting from logically incoherent treatment of inapplicable data (Maddison, 1993). We also present the results of tree searches with the algorithm described by Brazeau et al. (2018), which correctly handles inapplicable data in a parsimony setting. Finally, we document how each character is most parsimoniously reconstructed on an optimal tree.

Supplementary figures and tables appear after the text.

Chapter 1

Phylogenetic dataset

Analysis was performed on a new matrix of 54 lophotrochozoan taxa, coded for 225 morphological characters (129 neomorphic, 96 transformational). The matrix can be viewed interactively at Morphobank (project 2800) [This dataset will be released on publication of the paper. Referee access is available by logging in to MorphoBank using the e-mail address and password given in the manuscript.]; a static version can be downloaded directly :

- raw.githubusercontent.com/ms609/hyoliths/master/mbank_X24932_6-15-2018_519.nex (Nexus format)
- raw.githubusercontent.com/ms609/hyoliths/master/mbank_X24932_6-15-2018_519.tnt (TNT format).

Taxa include sipunculans and molluscs, which have previously been interpreted as having affinities with hyoliths. Other lophotrochozoan groups help to constrain the outgroup topology, and a diversity of brachiozoans helps to resolve the position of hyoliths within this group.

Characters are coded following the recommendations of Brazeau et al. (2018):

- We have employed reductive coding, using a distinct state to mark character inapplicability. Character specifications follow the structural syntax of Sereno (2007) in order to highlight ontological dependence between characters and emphasize the structure of the dataset.
- We have distinguished between neomorphic and transformational characters (*sensu* Sereno, 2007) by reserving the token 0 to refer to the absence of a neomorphic (i.e. presence/absence) character. The states of transformational characters (i.e. characters that describe a property of a feature) are represented by the tokens 1, 2, 3, ...
- We code the absence of neomorphic ontologically dependent characters (*sensu* Vogt, 2017) as absence, rather than inapplicability.

The complete dataset comprises 12150 character codings, of which 1133 are inapplicable and 4975 were positive statements (i.e. neither ambiguous nor inapplicable). This latter value, the amount and quality of data that *is* coded, is more instructive than the number of cells that are ambiguous (Wiens, 1998, 2003). Of the 225 characters, the number that were coded with an applicable token for each taxon is:

<u>Acanthotretella spinosa</u>	70	<u>Gasconsia</u>	70	<u>Novocrania</u>	186
<u>Alisina</u>	84	<u>Glyptoria</u>	73	<u>Orthis</u>	70
<u>Amathia</u>	157	<u>Halkieria evangelista</u>	65	<u>Paramicrocornus</u>	57
<u>Antigonambonites planus</u>	85	<u>Haplophrentis carinatus</u>	82	<u>Paterimitra</u>	67
<u>Askepasma toddense</u>	78	<u>Heliomedusa orienta</u>	67	<u>Pauxillites</u>	56
<u>Bactrotheca</u>	53	<u>Kutorgina chengjiangensis</u>	84	<u>Pedunculotheca diana</u>	63
<u>Botsfordia</u>	75	<u>Lingula</u>	205	<u>Pelagodiscus atlanticus</u>	166
<u>Clupeafumosus socialis</u>	76	<u>Lingulellotreta malongensis</u>	87	<u>Phoronis</u>	169
<u>Conotheca</u>	60	<u>Lingulosacculus</u>	60	<u>Salanygolina</u>	79
<u>Coolinia pecten</u>	80	<u>Longtancunella chengjiangensis</u>	61	<u>Serpula</u>	170
<u>Cotyledion tylodes</u>	65	<u>Loxosomella</u>	164	<u>Siphonobolus priscus</u>	74
<u>Craniops</u>	66	<u>Maxilites</u>	61	<u>Sipunculus</u>	168
<u>Cupitheca holocyclata</u>	63	<u>Mickwitzia muralensis</u>	72	<u>Terebratulina</u>	184
<u>Dailyatia</u>	55	<u>Micrina</u>	71	<u>Tomteluva perturbata</u>	58
<u>Dentalium</u>	169	<u>Micromitra</u>	81	<u>Tonicella</u>	188
<u>Eccentrotheca</u>	54	<u>Mummpikia nuda</u>	55	<u>Ussunia</u>	53
<u>Eoobolus</u>	81	<u>Namacalathus</u>	59	<u>Wiwaxia corrugata</u>	75
<u>Flustra</u>	168	<u>Nisusia sulcata</u>	80	<u>Yuganotheca elegans</u>	56

Chapter 2

Fitch parsimony

Parsimony search with the Fitch (1971) algorithm was conducted in TNT v1.5 (Goloboff and Catalano, 2016) using Ratchet and tree drifting heuristics (Goloboff, 1999; Nixon, 1999), repeating the search until the optimal score had been hit by 1500 independent searches:

```
xmult:rat10 drift10 hits 1500 level 4 chklevel 5;
```

Searches were conducted under equal weights and results saved to file:

```
piwe-; xmult; /* Conduct search with equal weighting */  
tsav *TNT/ew.tre;sav;tsav/; /* Save results to file */
```

Node support was estimated by calculating the proportion of jackknife replicates in which each group occurred, using 5000 symmetric resampling iterations, following the recommendations of Kopuchian and Ramírez (2010) and Simmons and Freudenstein (2011).

```
var: nt; /* Define a variable to track tree address */  
nelsen *; /* Generate strict consensus tree */  
set nt ntrees; ttag=; /* Prepare for resampling */  
resample=sym 5000 frequency from 'nt'; /* Symmetric resampling, counting frequencies */  
log TNT/ew.sym; ttag/; log/; /* Write results to log */  
keep 0; ttag-; hold 10000; /* Clear memory */
```

Further searches were conducted under extended implied weighting (Goloboff, 1997, 2014), under the concavity constants 2, 3, 4.5, 7, 10.5, 16 and 24:

```
xpiwe=; /* Enable extended implied weighting */  
piwe=2; xmult; /* Conduct analysis at k = 2 */  
tsav *TNT/xpiwe2.tre; sav; tsav/; /* Save results to file */  
nelsen *; set nt ntrees; ttag=; /* Prepare for resampling */  
resample=frequency from 'nt'; /* Symmetric resampling */  
log TNT/ew.sym; ttag/; log/; /* Write results to log */  
keep 0; ttag-; hold 10000; /* Clear memory */  
/* Repeat this block for each value of k */
```

Results can be replicated by:

- **Downloading the data in TNT format** raw.githubusercontent.com/ms609/hyoliths/master/mbank_X24932_6-15-2018_519.tnt
- Save the script above to the same directory, with the filename **tnt.run**.
- Open TNT, type **piwe=** before you load the downloaded dataset (to enable extended implied weighting), then type **tnt** into the command box to run the script.
- We acknowledge the Willi Hennig Society for their sponsorship of the TNT software.

2.1 Results

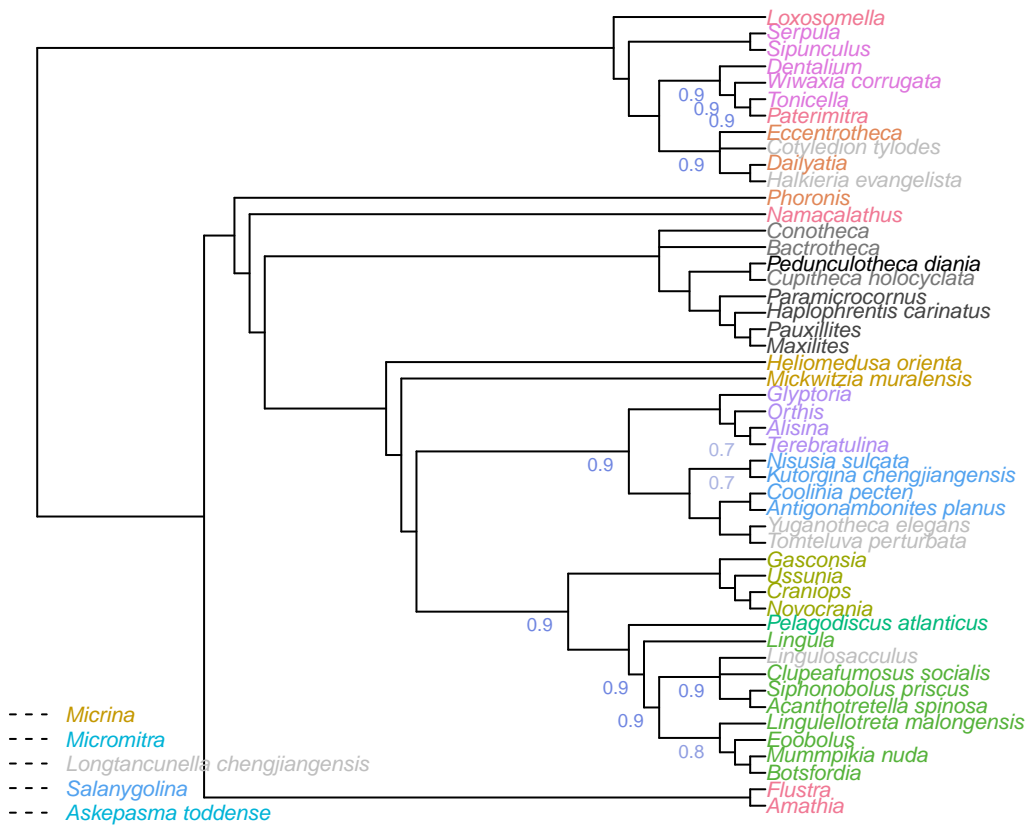


Figure 2.1: Majority-rule consensus of all trees that are optimal under $2 \leq k \leq 24$.

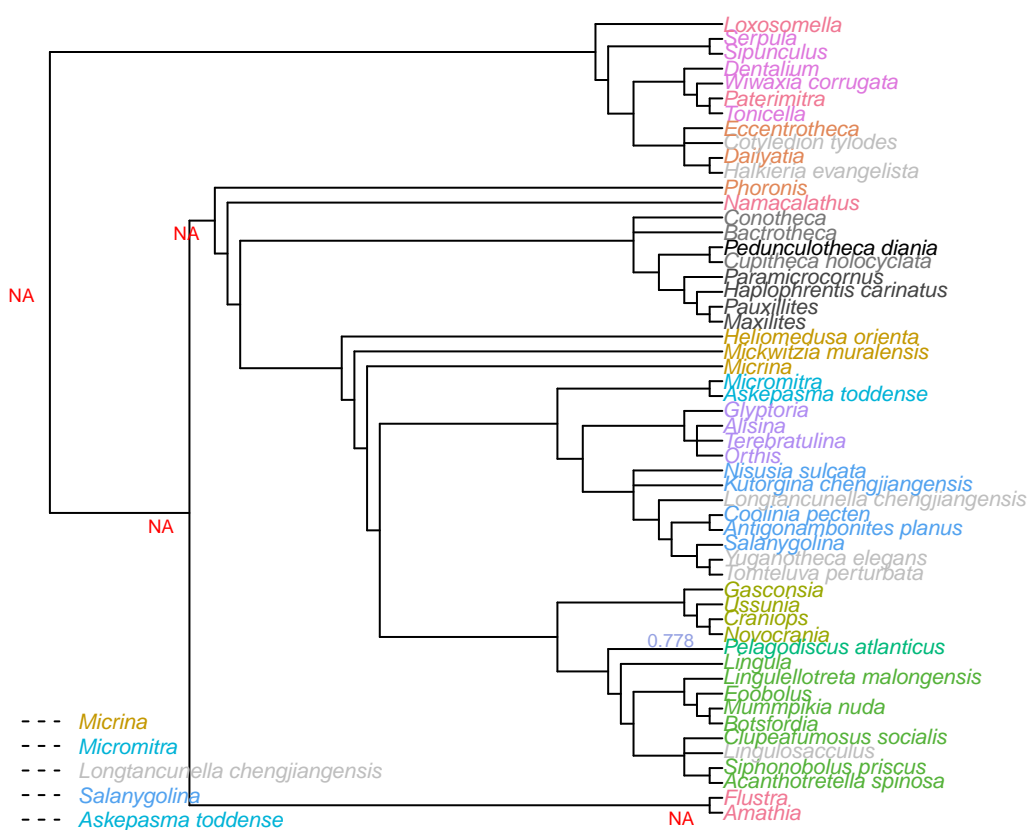


Figure 2.2: Majority-rule consensus of all trees that are optimal under $2 \leq k \leq 24$.

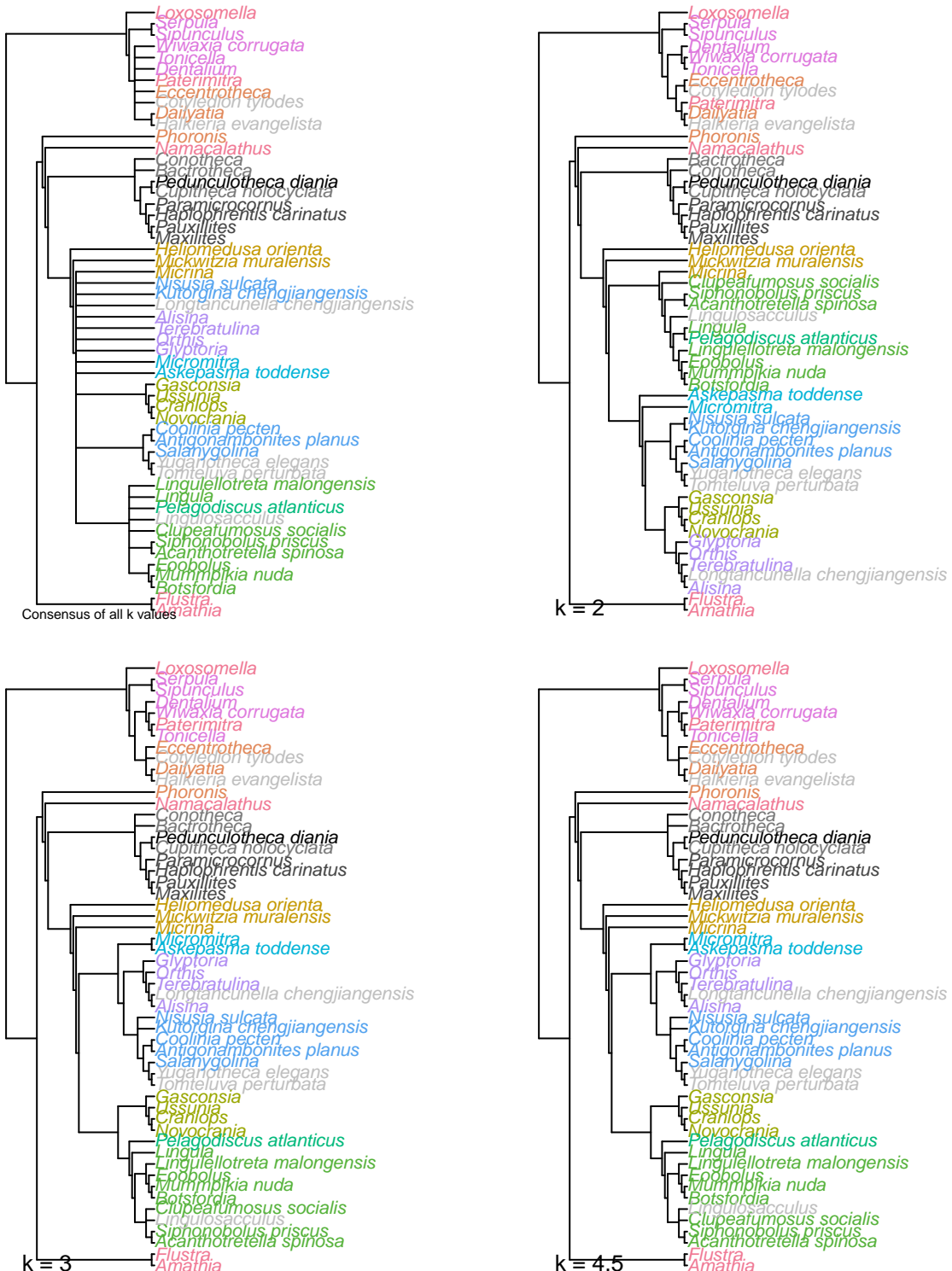


Figure 2.3: Strict consensus of all trees recovered by TNT using Fitch parsimony with implied weighting at all values of k , and at the individual values $k = 2, 3$ and 4.5 . The strict consensus of all implied weights runs is not very well resolved, largely due to an unusual optimal tree at $k = 2$, which obscures a consistent set of relationships between the remaining taxa.

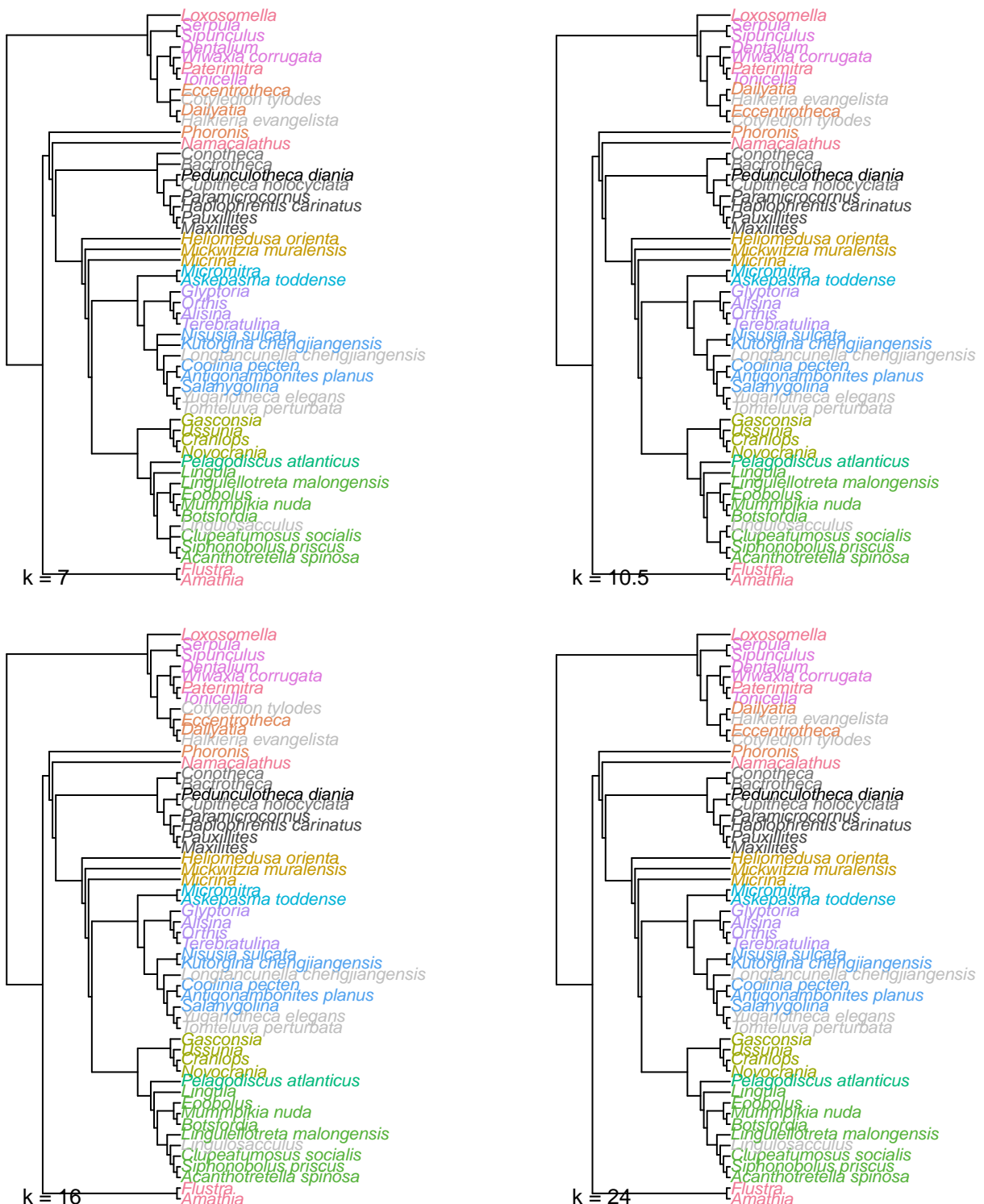


Figure 2.4: Strict consensus of all trees recovered by TNT using Fitch parsimony with implied weighting, at $k = 7, 10.5, 16$ and 24 .

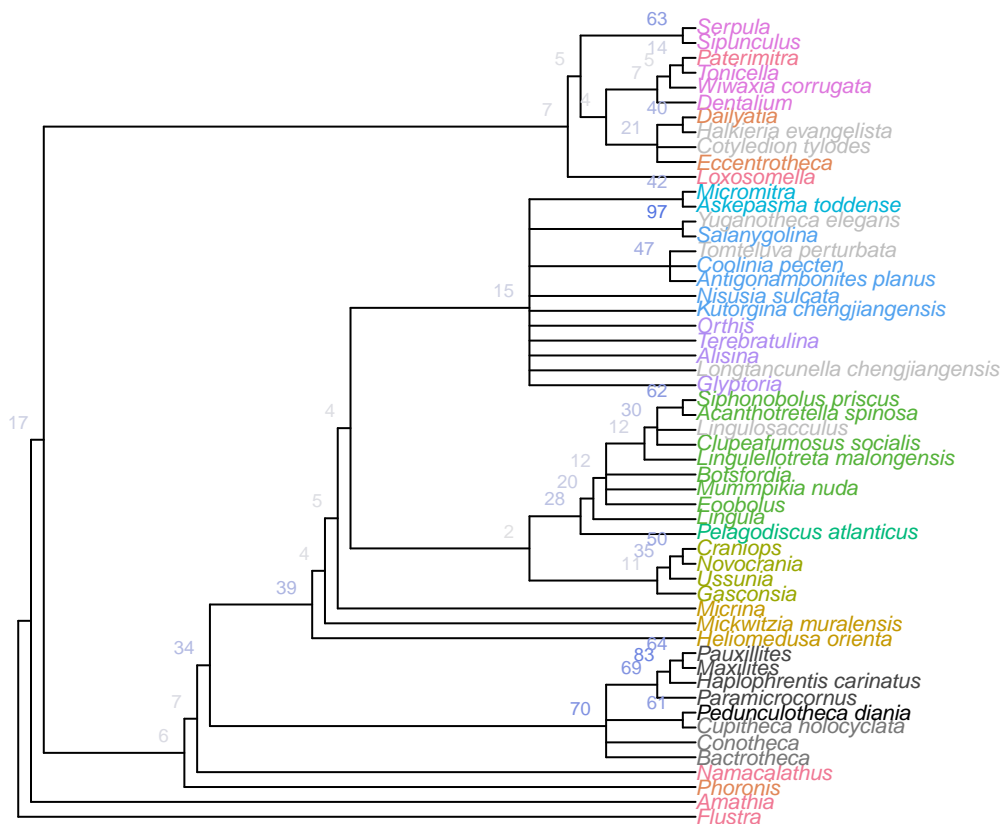


Figure 2.5: Consensus of all trees obtained using equally weighted Fitch parsimony in TNT. Nodes labelled with jackknife frequencies.

Chapter 3

Bayesian analysis

Bayesian search was conducted in MrBayes v3.2.6 (Ronquist et al., 2012) using the Mk model (Lewis, 2001) with gamma-distributed rate variation across characters:

```
lset coding=variable rates=gamma;
```

Branch length was drawn from a dirichlet prior distribution, which is less informative than an exponential model (Rannala et al., 2012), but requires a prior mean tree length within about two orders of magnitude of the true value (Zhang et al., 2012). To satisfy this latter criterion, we specified the prior mean tree length to be equal to the length of the most parsimonious tree under equal weights, using a Dirichlet prior with $\alpha_T = 1$, $\beta_T = 1/(equal\ weights\ tree\ length/number\ of\ characters)$, $\alpha = c = 1$:

```
prset brlenspr = unconstrained: gammadir(1, 0.35, 1, 1);
```

Neomorphic and transformational characters (*sensu* Sereno, 2007) were allocated to two separate partitions whose proportion of invariant characters and gamma shape parameters were allowed to vary independently:

```
charset Neomorphic = 1 6 7 9 10 15 18 19 20 21 22 24 26 29 30 34 35 37 38 40 43 44 45 48 49 53  
54 55 56 57 58 59 60 61 65 66 68 69 71 76 78 79 80 81 83 86 87 88 91 92 93 94 97 98 99 100 101  
102 106 108 109 111 118 119 121 122 125 126 129 136 137 138 139 140 142 143 144 145 148 150  
151 153 154 155 156 157 158 160 164 168 170 174 175 176 177 179 180 181 182 183 184 185 186  
187 188 190 192 193 196 199 202 203 204 205 206 207 209 210 211 212 214 215 216 217 218 219  
220 222 225;
```

```
charset Transformational = 2 3 4 5 8 11 12 13 14 16 17 23 25 27 28 31 32 33 36 39 41 42 46 47  
50 51 52 62 63 64 67 70 72 73 74 75 77 82 84 85 89 90 95 96 103 104 105 107 110 112 113 114  
115 116 117 120 123 124 127 128 130 131 132 133 134 135 141 146 147 149 152 159 161 162 163  
165 166 167 169 171 172 173 178 189 191 194 195 197 198 200 201 208 213 221 223 224;
```

```
partition chartype = 2: Neomorphic, Transformational;
```

```
set partition = chartype;
```

```
unlink shape=(all) pinvar=(all);
```

Neomorphic characters were not assumed to have a symmetrical transition rate – that is, the probability of the absent → present transition was allowed to differ from that of the present → absent transition, being drawn from a uniform prior:

```
prset applyto=(1) symdirhyperpr=fixed(1.0);
```

The rate of variation in neomorphic characters was also allowed to vary from that of transformational characters:

```
prset applyto=(1) ratepr=variable;
```

Loxosomella was selected as an outgroup:

```
outgroup Loxosomella;
```

Four MrBayes runs were executed, each sampling eight chains for 5 000 000 generations, with samples taken every 500 generations. The first 10% of samples were discarded as burn-in.

```
mcmcp ngen=5000000 samplefreq=500 nruns=4 nchains=8 burninfrac=0.1;
```

A posterior tree topology was derived from the combined posterior sample of all runs. Convergence was indicated by PSRF = 1.00 and an estimated sample size of > 200 for each parameter. Nodes are labelled with posterior probabilities; recall that caution must be applied when interpreting these values (Yang and Zhu, 2018).

The Nexus file used to generate these results in MrBayes can be raw.githubusercontent.com/ms609/hyoliths/master/MrBayes/nexus.nex and run in MrBayes by typing `exe path/to/download`.

3.1 Parameter estimates

Parameter	Mean	Variance	minESS	avgESS	PSRF
TL{all}	9.980	0.50100	5440	5970	0.99999
m{1}	0.462	0.00265	3100	3720	0.99999

3.2 Results

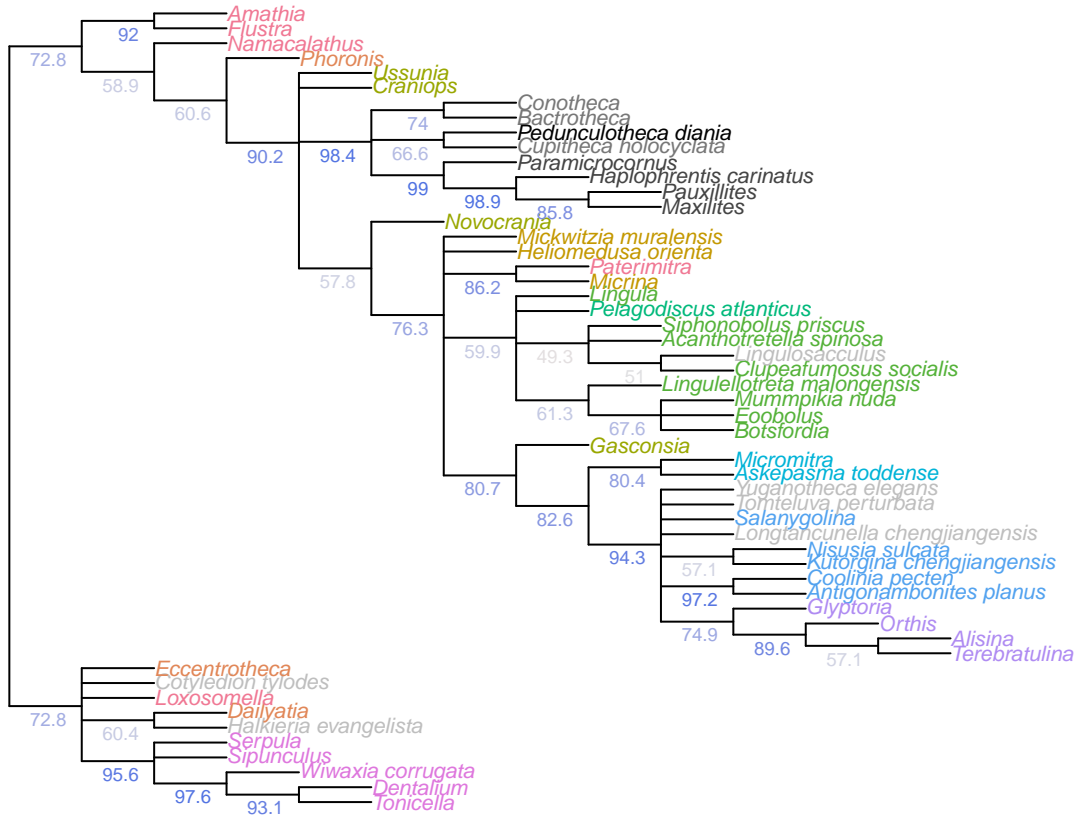


Figure 3.1: Results of Bayesian analysis, posterior probability > 50%, all taxa

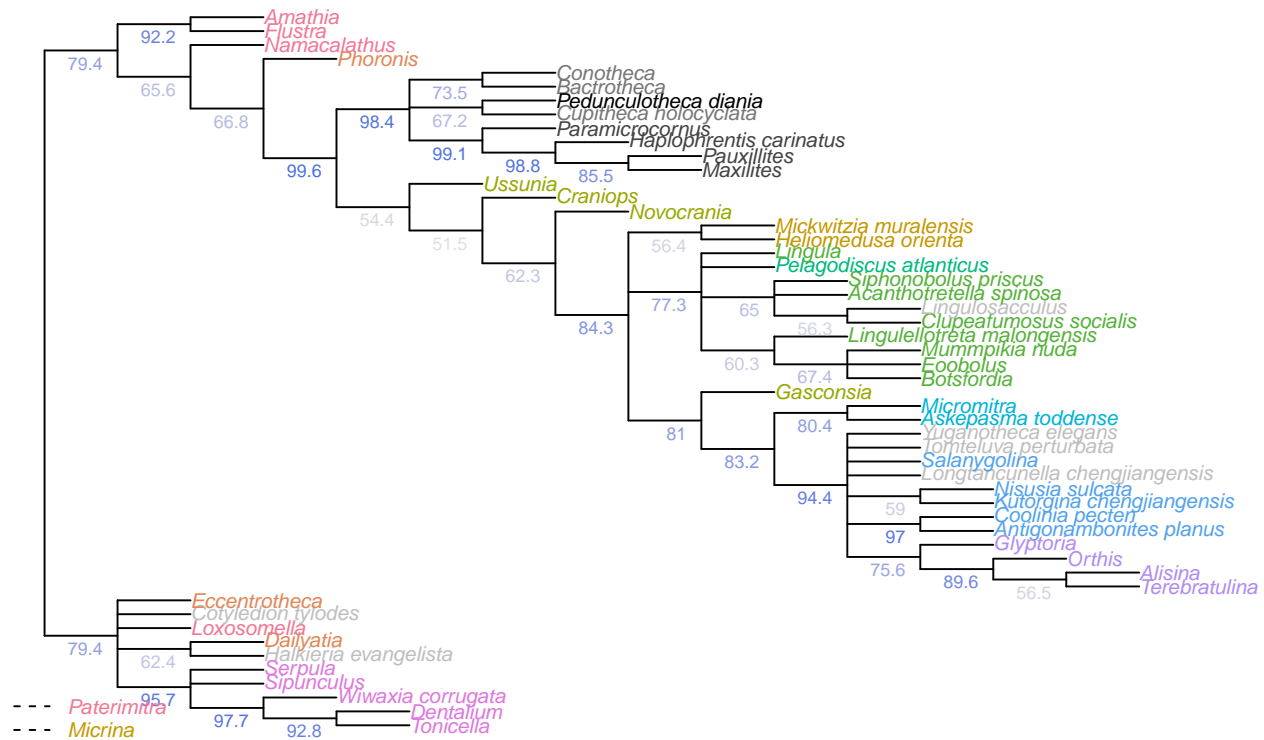


Figure 3.2: Results of Bayesian analysis, posterior probability > 50%, wildcard taxa pruned

Chapter 4

Corrected parsimony

The phylogenetic dataset contains a considerable proportion of inapplicable codings ($1133/12150 = 9.3\%$ of tokens), which are known to introduce error and bias to phylogenetic reconstruction when the Fitch algorithm is employed (Maddison, 1993; Brazeau et al., 2018). As such, we employed a new tree-scoring algorithm that correctly handles inapplicable data (Brazeau et al., 2018), implemented in the *MorphyLib* C library (Brazeau et al., 2017). We employed the R package *TreeSearch* v0.1.2 (Smith, 2018) to conduct phylogenetic tree search with this algorithm.

4.1 Search parameters

Heuristic searches were conducted using the parsimony ratchet (Nixon, 1999) under equal and implied weights (Goloboff, 1997). The consensus tree presented in the main manuscript represents a strict consensus of all trees that are most parsimonious under one or more of the concavity constants (k) 2, 3, 4.5, 7, 10.5, 16 and 24, an approach that has been shown to produce higher accuracy (i.e. more nodes and quartets resolved correctly) than equal weights at any given level of precision (Smith, 2017).

4.2 Analysis

The R commands used to conduct the analysis are reproduced below. The results can most readily be replicated using the R markdown files (.Rmd) used to generate these pages: in Rstudio, run raw.githubusercontent.com/ms609/hyoliths/master/index.Rmd, then run each block in raw.githubusercontent.com/ms609/hyoliths/master/14_TreeSearch.Rmd. The complete analysis will take several hours.

4.2.1 Initialize and load data

```
# Load data from locally downloaded copy of MorphoBank matrix
my_data <- ReadAsPhyDat(nexusFile)
my_data[ignored_taxa] <- NULL
iw_data <- PrepareDataIW(my_data)
```

4.2.2 Generate starting tree

Start by quickly rearranging a neighbour-joining tree, rooted on the outgroup.

```
nj.tree <- NJTree(my_data)
rooted.tree <- EnforceOutgroup(nj.tree, outgroup)
start.tree <- TreeSearch(tree=rooted.tree, dataset=my_data, maxIter=3000,
                        EdgeSwapper=RootedNNISwap, verbosity=0)
```

4.2.3 Implied weights analysis

The position of the root does not affect tree score, so we keep it fixed (using RootedXXXSwap functions) to avoid unnecessary swaps.

```
for (k in kValues) {
  iw.tree <- IW Ratchet(start.tree, iw_data, concavity=k,
                         ratchHits = 20, ratchIter=4000, searchHits=56,
                         swappers=list(RootedTBRSwap, RootedSPRSwap, RootedNNISwap),
                         verbosity=0L)
  score <- IWScore(iw.tree, iw_data, concavity=k)
  # Write a single best tree
  write.nexus(iw.tree,
              file=paste0("TreeSearch/hy_iw_k", k, "_",
                          signif(score, 5), ".nex", collapse=''))
  
  iw.consensus <- IW RatchetConsensus(iw.tree, iw_data, concavity=k,
                                         swappers=list(RootedTBRSwap, RootedNNISwap),
                                         searchHits=55, searchIter=4000, nSearch=250, verbosity=0L)
  write.nexus(iw.consensus,
              file=paste0("TreeSearch/hy_iw_k", k, "_",
                          signif(IWScore(iw.tree, iw_data, concavity=k), 5),
                          ".all.nex", collapse=''))
}
```

4.2.4 Equal weights analysis

```
ew.tree <- Ratchet(start.tree, my_data, verbosity=0L,
                     ratchHits = 20, ratchIter=4000, searchHits=55, # ratchHits = 20 not enough
                     swappers=list(RootedTBRSwap, RootedSPRSwap, RootedNNISwap))
ew.consensus <- RatchetConsensus(ew.tree, my_data, nSearch=250, searchHits = 85,
                                   swappers=list(RootedTBRSwap, RootedNNISwap),
                                   verbosity=0L)
write.nexus(ew.consensus, file=paste0(collapse=' ', "TreeSearch/hy_ew_",
                                       Fitch(ew.tree, my_data), ".nex"))
```

4.3 Results

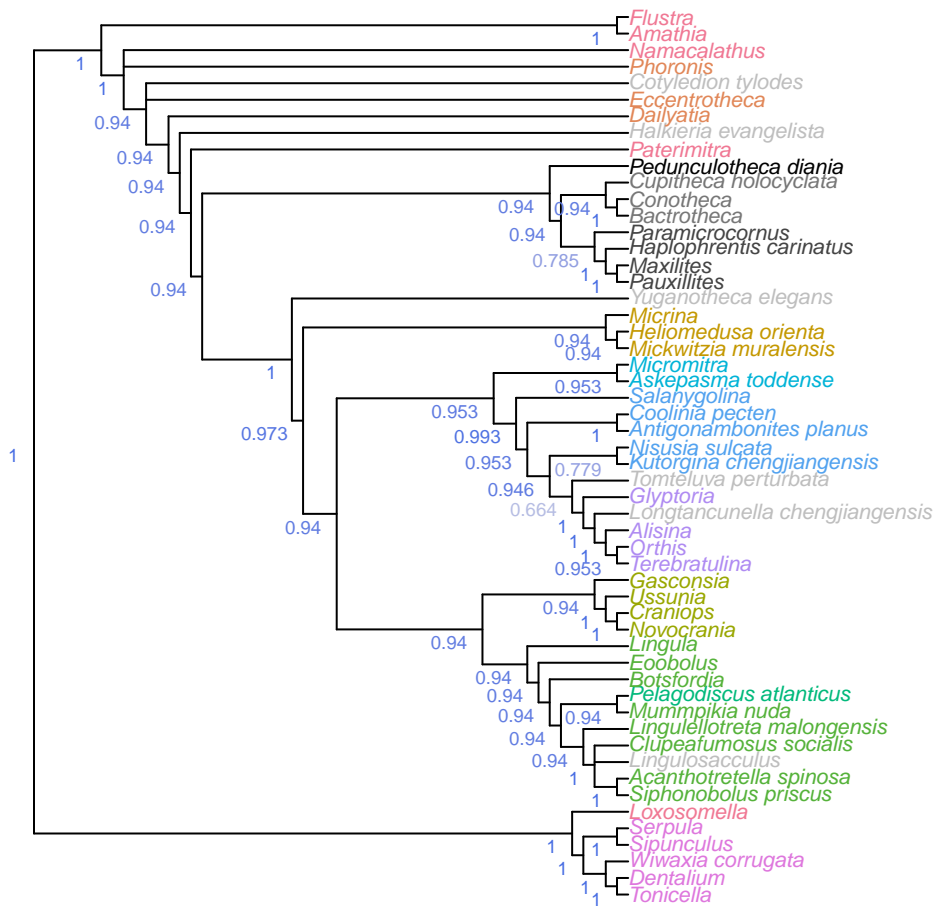


Figure 4.1: Consensus of all parsimony trees, under equal and implied weights. Node labels denote the frequency of each clade in most parsimonious trees under all analytical conditions.

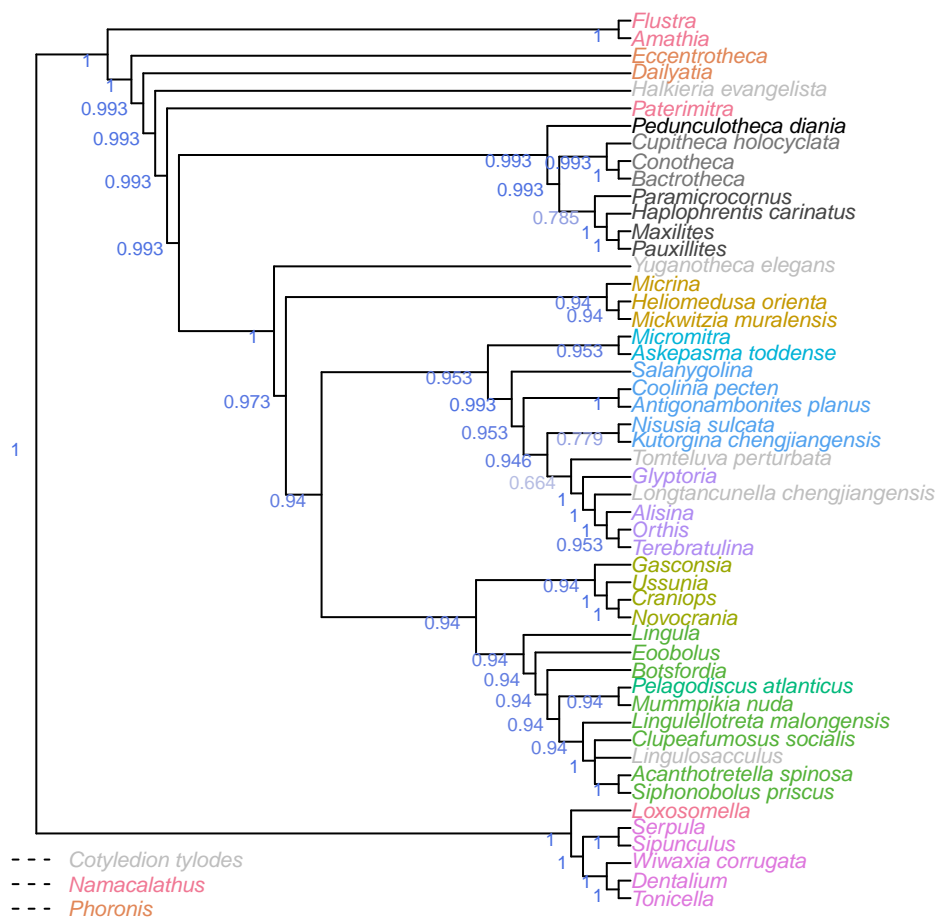


Figure 4.2: Consensus of same trees, with taxa pruned before constructing consensus to give context to clade support. Node labels denote the frequency of each clade in most parsimonious trees under all analytical conditions.

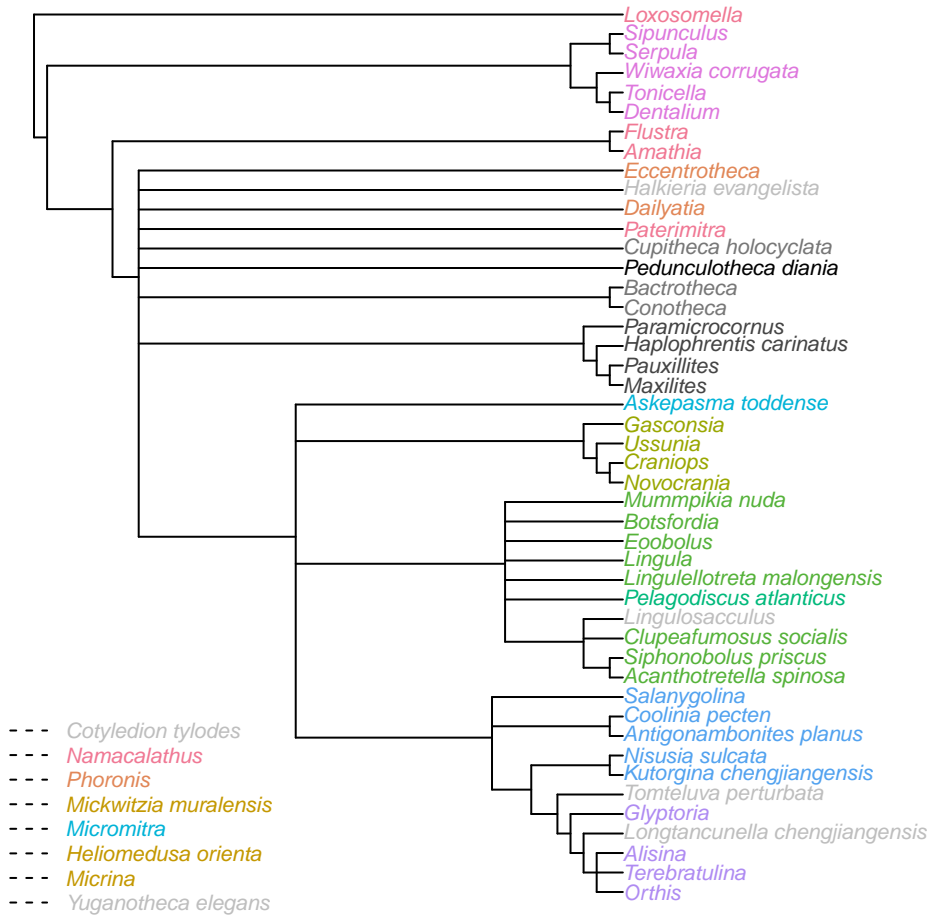


Figure 4.3: Strict consensus of implied weights analyses at all values of k . Wildcard taxa have been excluded from the consensus tree shown above to improve resolution.

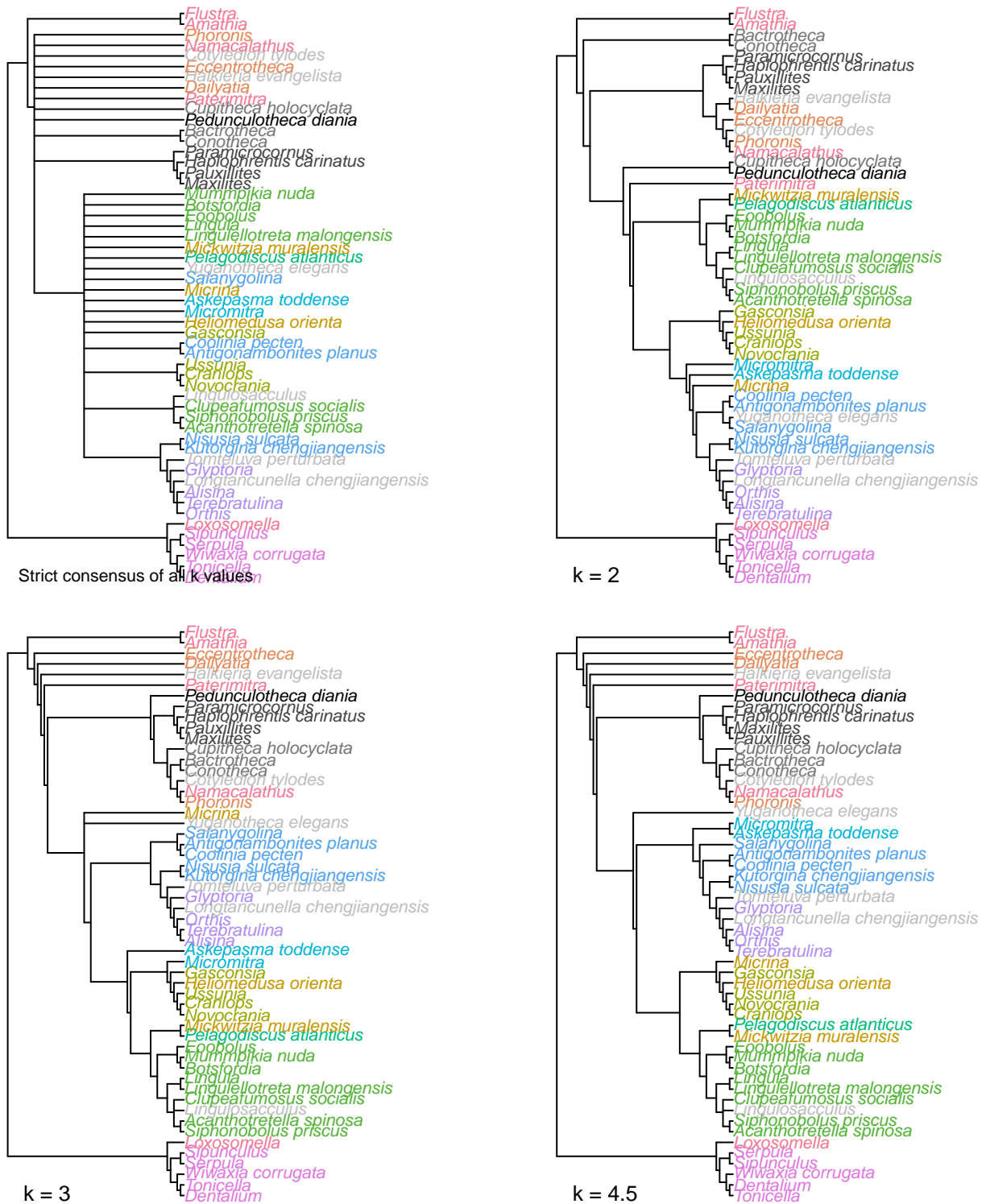
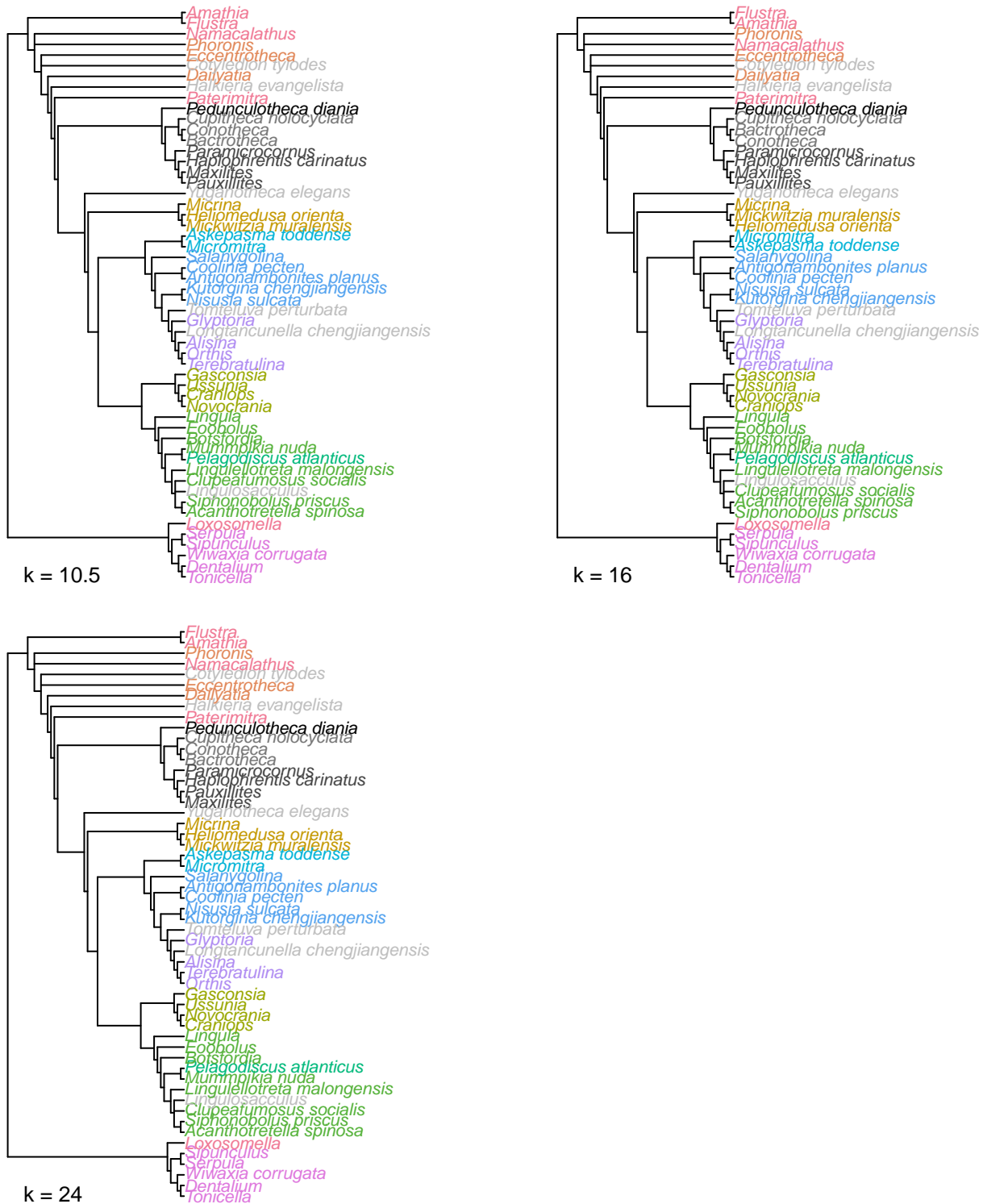


Figure 4.4: Strict consensus trees of implied weights analyses at all values of k , and at the individual values $k = 2, 3$ and 4.5 .

```
##  
## > Results not available for panel 4
```

Figure 4.5: Strict consensus trees of implied weights analyses at $k = 7, 10.5, 16$ and 24 .

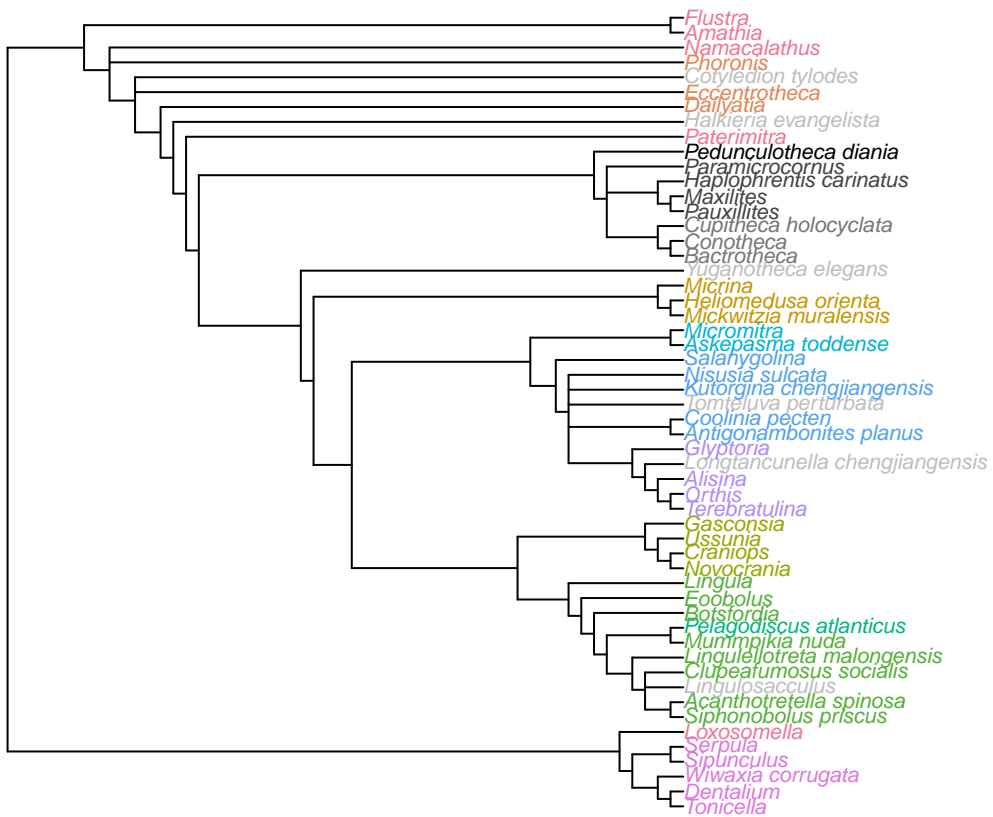


Figure 4.6: Strict consensus of most parsimonious trees under equally weighted parsimony

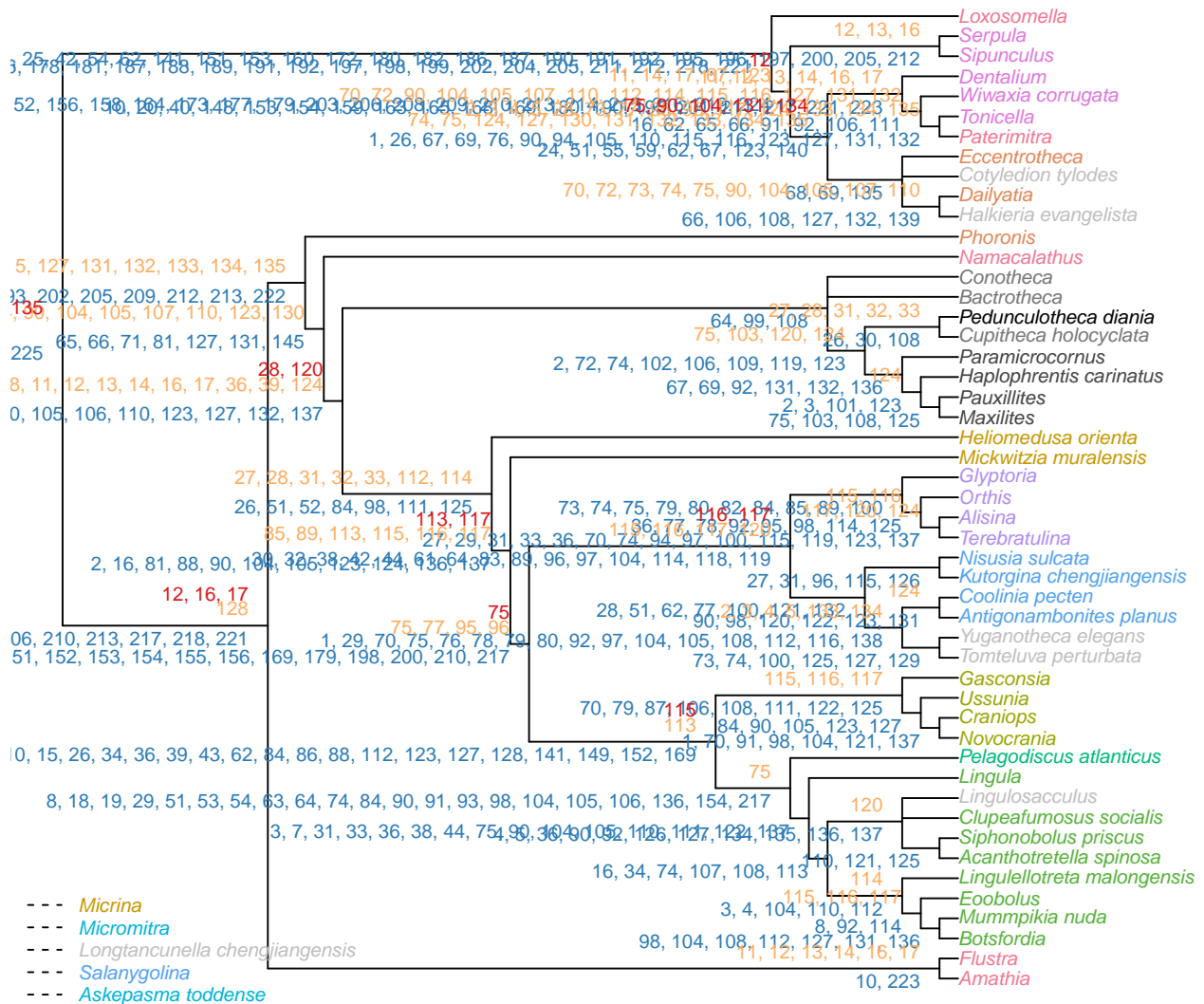
Chapter 5

Character reconstructions

This page provides definitions for each of the characters in our matrix, and justifies codings in particular taxa where relevant. Further citations for codings that are not discussed in the text can be viewed by browsing the morphological dataset on MorphoBank (project 2800). [This dataset will be released on publication of the paper. Referee access is available by logging in to MorphoBank using the e-mail address and password given in the manuscript.]

Alongside its definition, each character has been mapped onto a tree. Here, we have arbitrarily selected one most parsimonious tree obtained under implied weighting, $k = 4.5$. Other trees can be viewed in the HTML version of this document at ms609.github.io/hyoliths. Each tip is labelled according to its coding in the matrix. These states have been used to reconstruct the condition of each internal node, using the parsimony method of Brazeau et al. (2018) as implemented in the *R* package *Inapp*.

We emphasize that different trees will give different reconstructions. The character mappings are not intended to definitively establish how each character evolved, but to help the reader quickly establish how each character has been coded, and to visualize at a glance how each character fits onto a given tree.



Chapter 6

Taxonomic implications

This section briefly places key features of our results in the context of previous phylogenetic hypotheses.

Outgroup We advise caution in the interpretation of outgroup relationships. Outgroup taxa include single representatives of diverse and ancient phyla, and are thus prone to long branch error (Parks and Goldman, 2014). The relationships of the lophotrochozoan phyla were not the primary object of this study, and have long resisted elucidation; this said, we have attempted to incorporate all morphological evidence that has been interpreted as informing relationships between these groups.

Brachiopod crown and stem group Crown- and stem-group terminology has great value in clarifying the early evolution of major lineages (Budd and Jensen, 2000; Carlson and Cohen, 2009). The crown group of a lineage is defined as the last common ancestor of all living members of a group, and all its descendants; the stem group as all taxa more closely related to the crown group than to any other extant taxon. In our selection of taxa, the brachiopod crown group corresponds to the last common ancestor of *Terebratulina*, *Novocrania*, *Pelagodiscus* and *Lingula*; the brachiopod stem group comprises anything between this node and the branching point of *Phoronis*, which marks the base of the Brachiozoan crown group.

Craniiforms Trimerellids are reconstructed as paraphyletic with respect to Craniiforms. This is consistent with the affinity commonly drawn between these groups (e.g. Williams et al., 2000), and helps to account for the stratigraphically late (Ordovician) appearance of Craniids in the fossil record. (Aragonite is underrepresented in early Palaeozoic strata due to taphonomic bias.)

The position of the craniiforms is not conclusively resolved; shell characters point to a relationship with the Rhynchonelliforms, which is countered by similarities between the spermatozoa of phoronids and terebratulids, indicating a craniiform + linguliform clade. This latter relationship is preferred by the majority of parsimony analyses, though a small subset of weighting parameters places the craniiform clade within the rhynchonelliforms instead.

The Bayesian results offer a more surprising interpretation that places the craniiforms as paraphyletic with respect to all other brachiopods, with *Gasconsia* representing the basalmost member of the Rhynchonellid lineage, upholding suggestions (Holmer et al., 2014) of a chileid rather than trimerellid affinity. To our knowledge, the hypothesis of a paraphyletic craniiform+trimerellid grade has never been proposed, and represents a poor fit to stratigraphic data; potentially it represents an artefact resulting from the incorrect handling of inapplicable data within the Mk model.

Rhynchonelliforms The position of kutoarginids within the rhynchonelliform stem lineage has been tricky to resolve (Holmer et al., 2018b); our results agree that they form a clade, but differ on their closest relatives; Fitch parsimony places them as sister to the Chileids; correcting for inapplicables places them sister to Rhynchonelliforms; and Bayesian analysis fails to distinguish between these two possibilities. These results are broadly in accord with previous proposals (Holmer et al., 2018a). The protorthid *Glyptoria* is the earliest diverging of the included rhynchonelliform lineages.

Salanygolina has been interpreted as a stem-group rhynchonelliform based on its combination of paterinid and chileate features (Holmer et al., 2009). Our results position *Salanygolina* as sister either to the Chileids or the Chileids + Rhynchonelliforms, corroborating this interpretation.

Basal rhynchonellids are characterized by a circular umbonal perforation in the ventral valve, associated with a colleplax. Partly on this basis, the aberrant taxa *Yuganotheca* and *Tomteluva* tend to plot close to the chileids under Fitch and Bayesian analysis, though a variety of positions in this region of the tree are equally plausible. The BGS method, in contrast, supports the interpretation of *Yuganotheca* as a stem-group brachiopod (Zhang et al., 2014).

Linguliforms The reconstruction of Linguloformea comprising Linguloidea as sister to Discinoidea is as expected. Lingulellotretids also sit within this linguliform grouping; a position in the phoronid stem lineage (advocated by Balthasar and Butterfield, 2009) is not upheld. Acrotretids and Siphonotretids form a clade with *Lingulosacculus*.

More novel is the reconstruction of the calcitic obolellid *Mummpikia* in the linguliform total group: a rhynchonelliform affinity has been assumed based on its calcitic mineralogy. This said, Balthasar (2008) has highlighted the similarities between obolellids and linguliform brachiopods, including sub- m vertical canals and the detailed configuration of the posterior shell margin. Our analysis upholds the case for a linguliform affinity for *Mummpikia*; a calcitic shell seemingly arose through an independent change within this taxon. As such, *Mummpikia* has no direct bearing on the origin of ‘Calciata’, save that shell mineralogy is perhaps less static than commonly assumed.

More generally, our results identify Class Obolellata as polyphyletic: *Alisina* (Trematobolidae) plots within Rhynchonellata; *Tomteluva* is harder to place, but tends to group with *Salanygolina* stemwards of the chileids.

Paterinids Paterinids have traditionally been placed within the Linguliforms on the basis of their phosphatic shell (Williams et al., 2007), which we identify as ancestral within the brachiopod crown group; consequently, our analysis places the paterinids within the Rhynchonelliforms instead. Characters supporting this position include the strophic hinge line, planar cardinal area, the absence of a pedicle nerve impression, and the morphology of the mantle canals.

More generally, although some lingulids can be found which share more generic characters (e.g. shell growth direction) with paterinids, the particular combination of characters exhibited in paterinids does not occur anywhere in the linguliform lineage, but is more similar to that of basal rhynchonelliforms, particularly *Salanygolina* (as noted by Holmer et al., 2009).

Tommotiids Tommotiids represent a basal grade, paraphyletic to phoronids and crown-group brachiopods, in line with previous interpretations.

Mickwitzia is consistently the most crownwards of the tommotiids, falling as sister to the brachiopod crown group (except in the Bayesian results, where they fall within the paraphyletic craniiform grade). *Mickwitzia* is closely related to *Micrina* and *Heliomedusa*, though the exact nature of this relationship varies from analysis to analysis. The latter affiliation reflects similarities emphasized by Holmer and Popov in Williams et al. (2007).

Dailyatia tends to plot closely with *Halkieria*, reflecting the similarity in the form of their proposed scleritome (Skovsted et al., 2015). Bayesian analysis recovers this pair as sister to annelids and molluscs; Fitch parsimony places them in the molluscan stem group. Inapplicable-corrected parsimony instead places these taxa as sister to hyoliths + brachiopods (cf. Zhao et al., 2017).

Hyoliths Within the hyoliths, orthothecids are consistently recovered as a grade that is paraphyletic to the hyolithids. Hyoliths as a whole are interpreted as stem-group Brachiopods, which refines the broader phylogenetic position proposed by Moysiuk et al. (2017). This is to say, they sit closer to brachiopods than the phoronids do, but no analysis places them within the Brachiopod crown group.

Tommotiids lie both stemwards (e.g. *Eccentrotheca*) and crownwards (*Mickwitzia*) of hyoliths, which thus represent derived tommotiids.

Supplementary Figures

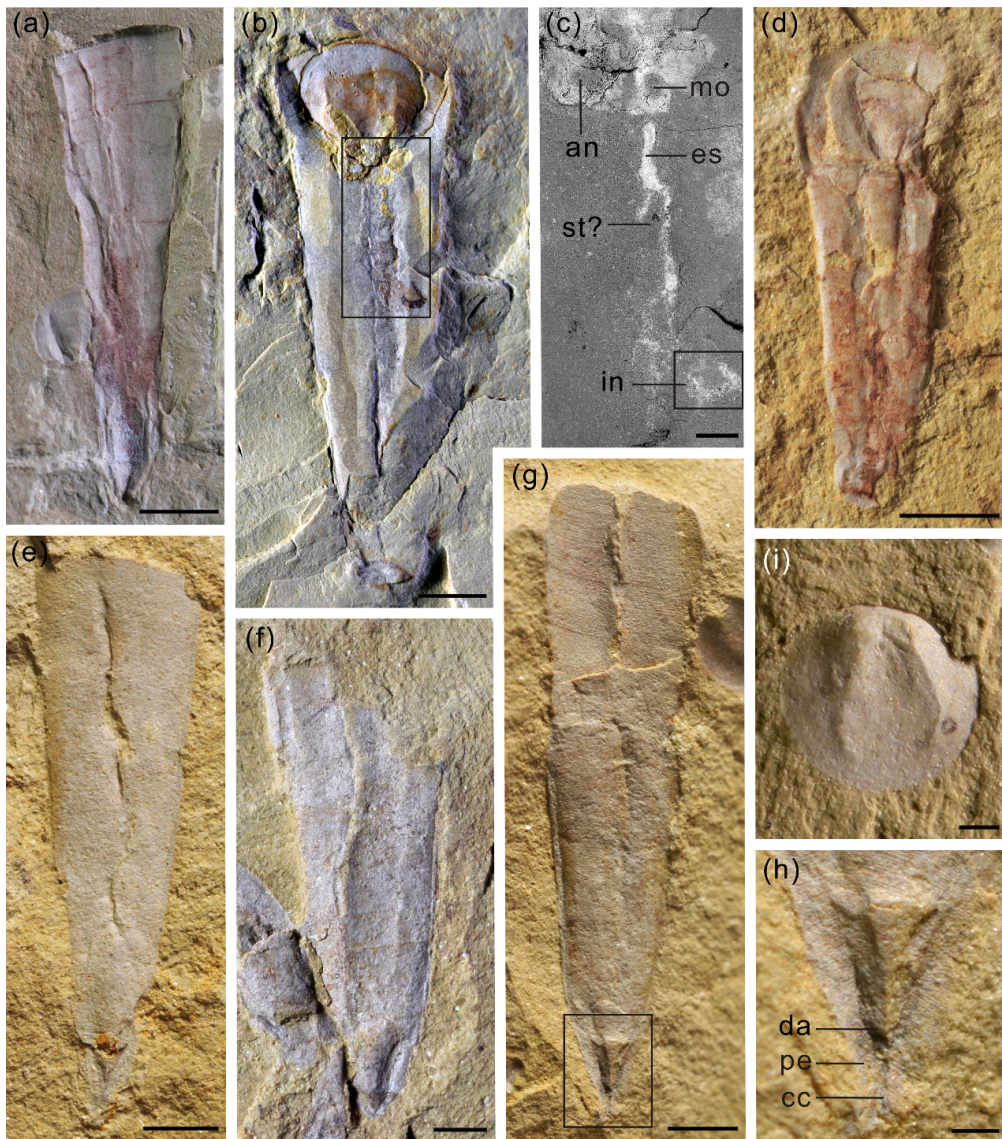


Fig. S1. *Pedunculotheca diania* Sun, Zhao et Zhu gen. et sp. nov. from the Chengjiang Biota, Yunnan Province, China. (a) NIGPAS 166601, external mould of dorsum with dorsal apex and pedicle foramen. (b) NIGPAS 166597, preserving conical shell, operculum and internal soft tissue, showing a compressed elliptic cross-section; backscatter electron micrograph of boxed region shown in (c). (d) NIGPAS 166599b, counterpart, juvenile conical shell with operculum showing two longitudinal ventral grooves and

circular larval shell. (e) NIGPAS 166602, conical shell with incomplete attachment structure. (f) NIGPAS 166598, broken shell with two ventral furrows and incomplete attachment structure. (g) NIGPAS 166596, incomplete shell with one medial ventral furrow and short attachment structure with coelomic cavity; detail of boxed region shown in (h). (i) NIGPAS 166603, exterior of operculum. Scale bars: 2mm (for a, b and e-g); 500 µm (for c, h and i).

Abbreviations: an = anus, cc = coelomic cavity, da = dorsal apex, es = esophagus, in = intestine, mo = mouth, pe = pedicle, st = stomach.

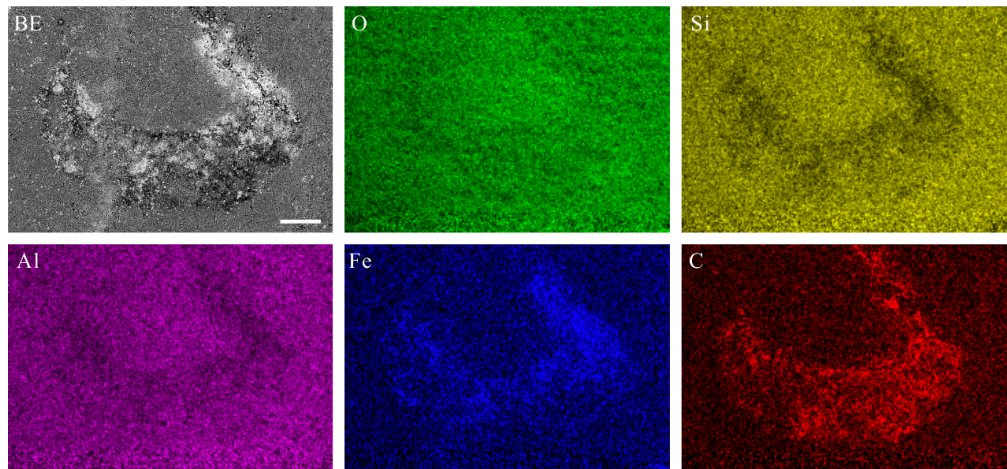


Fig. S2. Elemental distribution in the gut of *Pedunculotheca diania* Sun, Zhao et Zhu gen. et sp. nov. NIGPAS 166597. Region corresponds to boxed region in Fig. S1c. Scale bar = 100 µm.

Abbreviations: BE = backscatter electron image, O = Oxygen, Si = Silicon, Al = Aluminium, Fe = Iron, C = Carbon.

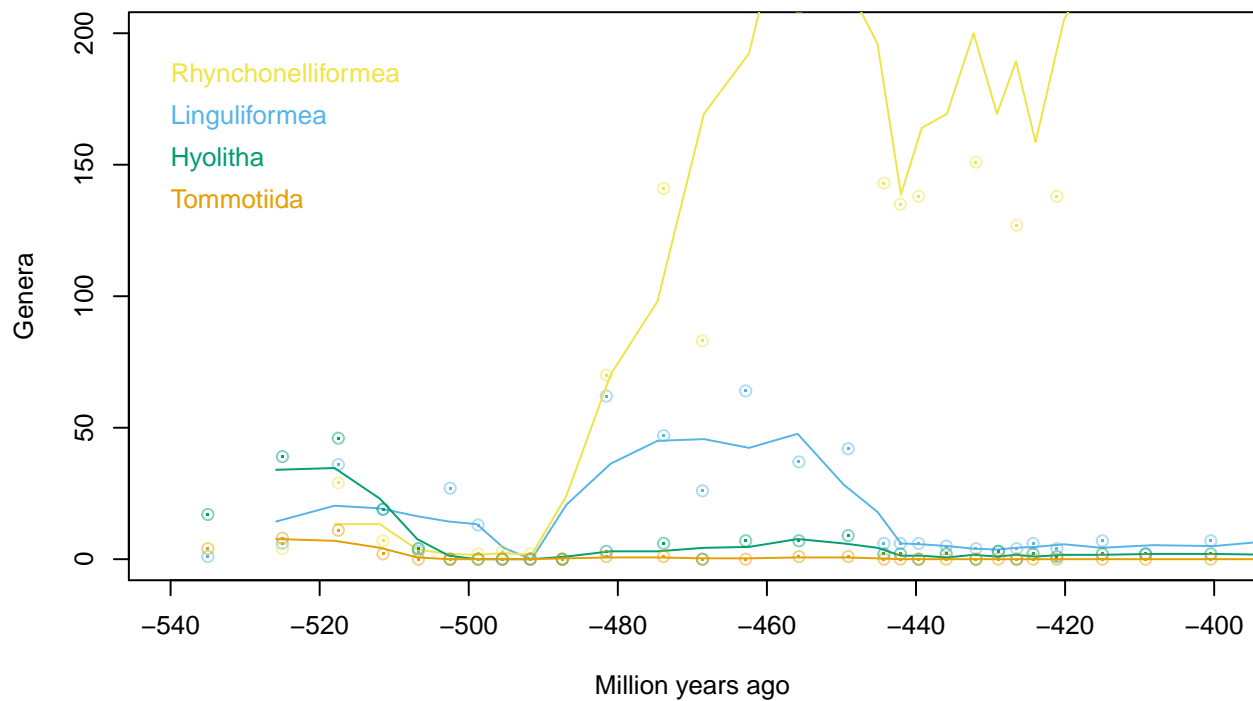


Fig. S3. Global diversity of brachiopods through the Paleozoic. Points represent number of genera reported in each time bin; lines represent rolling mean diversity over three consecutive time bins. Data from Paleobiology database.

Supplementary Table

NIGPAS Specimen numbers	Fossil locality	Coordinates
166593, 166617	Shankou Village, Anning	24°49'53" N, 102°24'47.9" E
166594, 166595	Yaoying Village, Wuding	25°36'01.2" N, 102°20'04.6" E
166596–166616	Ma'anshan Village, Chengjiang	24°40'37.2" N, 102°58'40.2" E

Table S1. Provenance of fossil material. Individuals from the Yaoying section are usually bigger, with a thicker body wall, and have a smaller ratio of apertural width to shell length than specimens from other areas. In the absence of other differentiating features, we consider these deviations to represent ecophenotypical variation within a single species, perhaps reflecting the increased energetics and predation pressure that accompany the shallower water depth reported at the Yaoying section (Zhao et al., 2012).

Bibliography

- Balthasar, U. (2008). *Mummpikia* gen. nov. and the origin of calcitic-shelled brachiopods. *Palaeontology*, 51(2):263–279, doi:10.1111/j.1475-4983.2008.00754.x.
- Balthasar, U. and Butterfield, N. J. (2009). Early Cambrian soft-shelled brachiopods as possible stem-group phoronids. *Acta Palaeontologica Polonica*, 54(2):307–314, doi:10.4202/app.2008.0042.
- Brazeau, M. D., Guillerme, T., and Smith, M. R. (2018). An algorithm for morphological phylogenetic analysis with inapplicable data. *Systematic Biology*, doi:10.1101/209775.
- Brazeau, M. D., Smith, M. R., and Guillerme, T. (2017). MorphyLib: a library for phylogenetic analysis of categorical trait data with inapplicability. *Zenodo*, doi:10.5281/zenodo.815371.
- Budd, G. E. and Jensen, S. (2000). A critical reappraisal of the fossil record of the bilaterian phyla. *Biological Reviews*, 75(2):253–295, doi:10.1111/j.1469-185X.1999.tb00046.x.
- Carlson, S. J. and Cohen, B. L. (2009). Separating the crown from the stem: defining Brachiopoda and Pan-Brachiopoda delineates stem-brachiopods. *Geological Society of America Annual Meeting Abstract Program*, 41:562.
- Fitch, W. M. (1971). Toward defining the course of evolution: minimum change for a specific tree topology. *Systematic Biology*, 20(4):406–416, doi:10.1093/sysbio/20.4.406.
- Goloboff, P. A. (1997). Self-weighted optimization: tree searches and character state reconstructions under implied transformation costs. *Cladistics*, 13(3):225–245, doi:10.1111/j.1096-0031.1997.tb00317.x.
- Goloboff, P. A. (1999). Analyzing large data sets in reasonable times: solutions for composite optima. *Cladistics*, 15(4):415–428, doi:10.1006/clad.1999.0122.
- Goloboff, P. A. (2014). Extended implied weighting. *Cladistics*, 30(3):260–272, doi:10.1111/cla.12047.
- Goloboff, P. A. and Catalano, S. A. (2016). TNT version 1.5, including a full implementation of phylogenetic morphometrics. *Cladistics*, 32(3):221–238, doi:10.1111/cla.12160.
- Holmer, L. E., Pettersson Stolk, P. S., Skovsted, C. B., Balthasar, U., and Popov, L. E. (2009). The enigmatic early Cambrian *Salanygolina* – A stem group of rhynchonelliform chileate brachiopods? *Palaeontology*, 52(1):1–10, doi:10.1111/j.1475-4983.2008.00831.x.
- Holmer, L. E., Popov, L. E., and Bassett, M. G. (2014). Ordovician–Silurian Chileida—first post-Cambrian records of an enigmatic group of Brachiopoda. *Journal of Paleontology*, 88(3):488–496, doi:10.1666/13-104.
- Holmer, L. E., Popov, L. E., Pour, M. G., Claybourn, T., Zhang, Z.-L., Brock, G. A., and Zhang, Z.-F. (2018a). Evolutionary significance of a middle Cambrian (Series 3) *in situ* occurrence of the pedunculate rhynchonelliform brachiopod *Nisusia sulcata*. *Lethaia*, doi:10.1111/let.12254.
- Holmer, L. E., Zhang, Z.-F., Topper, T. P., Popov, L. E., and Claybourn, T. M. (2018b). The attachment strategies of Cambrian kutorginate brachiopods: the curious case of two pedicle openings and their phylogenetic significance. *Journal of Paleontology*, 92(1):33–39, doi:10.1017/jpa.2017.76.

- Kopuchian, C. and Ramírez, M. J. (2010). Behaviour of resampling methods under different weighting schemes, measures and variable resampling strengths. *Cladistics*, 26(1):86–97, doi:10.1111/j.1096-0031.2009.00269.x.
- Lewis, P. O. (2001). A likelihood approach to estimating phylogeny from discrete morphological character data. *Systematic Biology*, 50(6):913–925, doi:10.1080/106351501753462876.
- Maddison, W. P. (1993). Missing data versus missing characters in phylogenetic analysis. *Systematic Biology*, 42(4):576–581, doi:10.1093/sysbio/42.4.576.
- Moysiuk, J., Smith, M. R., and Caron, J.-B. (2017). Hyoliths are Palaeozoic lophophorates. *Nature*, 541(7637):394–397, doi:10.1038/nature20804.
- Nixon, K. C. (1999). The Parsimony Ratchet, a new method for rapid parsimony analysis. *Cladistics*, 15(4):407–414, doi:10.1111/j.1096-0031.1999.tb00277.x.
- Parks, S. L. and Goldman, N. (2014). Maximum Likelihood inference of small trees in the presence of long branches. *Systematic Biology*, 63(5):798–811, doi:10.1093/sysbio/syu044.
- Rannala, B., Zhu, T.-Q., and Yang, Z.-H. (2012). Tail paradox, partial identifiability, and influential priors in Bayesian branch length inference. *Molecular Biology and Evolution*, 29(1):325–335, doi:10.1093/molbev/msr210.
- Ronquist, F., Teslenko, M., van der Mark, P., Ayres, D. L., Darling, A., Hohna, S., Larget, B., Liu, L., Suchard, M. A., and Huelsenbeck, J. P. (2012). MrBayes 3.2: efficient Bayesian phylogenetic inference and model choice across a large model space. *Systematic Biology*, 61(3):539–42, doi:10.1093/sysbio/sys029.
- Sereno, P. C. (2007). Logical basis for morphological characters in phylogenetics. *Cladistics*, 23(6):565–587, doi:10.1111/j.1096-0031.2007.00161.x.
- Simmons, M. P. and Freudenstein, J. V. (2011). Spurious 99% bootstrap and jackknife support for unsupported clades. *Molecular Phylogenetics and Evolution*, 61(1):177–191, doi:10.1016/j.ympev.2011.06.003.
- Skovsted, C. B., Betts, M. J., Topper, T. P., and Brock, G. A. (2015). The early Cambrian tommotiid genus *Dailyatia* from South Australia. *Memoirs of the Association of Australasian Palaeontologists*, 48(1):1–117.
- Smith, M. R. (2017). Quantifying and visualising divergence between pairs of phylogenetic trees: implications for phylogenetic reconstruction. *bioRxiv*, doi:10.1101/227942.
- Smith, M. R. (2018). TreeSearch: phylogenetic tree search using custom optimality criteria.
- Sun, H.-J., Smith, M. R., Zeng, H., Zhao, F.-C., Li, G.-X., and Zhu, M.-Y. (2018). Hyoliths with pedicles constrain the origin of the brachiopod body plan. page submitted.
- Vogt, L. (2017). The logical basis for coding ontologically dependent characters. *Cladistics*, doi:10.1111/cla.12209.
- Wiens, J. J. (1998). Does adding characters with missing data increase or decrease phylogenetic accuracy? *Systematic Biology*, 47(4):625–640, doi:10.1080/106351598260635.
- Wiens, J. J. (2003). Missing data, incomplete taxa, and phylogenetic accuracy. *Systematic Biology*, 52(4):528–538, doi:10.1080/10635150390218330.
- Williams, A., Carlson, S. J., Brunton, C. H. C., Holmer, L. E., Popov, L. E., Mergl, M., Laurie, J. R., Bassett, M. G., Cocks, L. R. M., Rong, J.-Y., Lazarev, S. S., Grant, R. E., Racheboeuf, P. R., Jin, Y.-G., Wardlaw, B. R., Harper, D. A. T., and Wright, A. D. (2000). Linguliformea, Craniiformea, and Rhynchonelliformea (part). In *Treatise on Invertebrate Paleontology, Part H, Brachiopoda (Revised)*, volume 2 & 3, pages 1–919. Geological Society of America & Paleontological Institute.

- Williams, A., Racheboeuf, P. R., Savage, N. M., Lee, D. E., Popov, L. E., Carlson, S. J., Logan, A., Lüter, C., Cusack, M., Curry, G. B., Wright, A. D., Harper, D. A. T., Cohen, B. L., Cocks, L. R. M., MacKinnon, D. I., Smirnova, T. N., Baker, P. G., Carter, J. L., Gourvennec, R., Mancenido, M. O., Brunton, C. H. C., Dong-Li, D.-S., Boucot, A. J., Bassett, M. G., Alvarez, F., Holmer, L. E., Mergl, M., Emig, C. C., Rubel, M., and Jia-Yu, J.-R. (2007). Supplement. In *Treatise on Invertebrate Paleontology, Part H, Brachiopoda (Revised)*, volume 6, pages 2321–3226. Geological Society of America & Paleontological Institute.
- Yang, Z. and Zhu, T. (2018). Bayesian selection of misspecified models is overconfident and may cause spurious posterior probabilities for phylogenetic trees. *Proceedings of the National Academy of Sciences*, 115(8):1854–1859, doi:10.1073/pnas.1712673115.
- Zhang, C., Rannala, B., and Yang, Z.-H. (2012). Robustness of compound Dirichlet priors for Bayesian inference of branch lengths. *Systematic Biology*, 61(5):779–84, doi:10.1093/sysbio/sys030.
- Zhang, Z.-F., Li, G.-X., Holmer, L. E., Brock, G. A., Balthasar, U., Skovsted, C. B., Fu, D.-J., Zhang, X.-L., Wang, H.-Z., Butler, A. D., Zhang, Z.-L., Cao, C.-Q., Han, J., Liu, J.-N., and Shu, D.-G. (2014). An early Cambrian agglutinated tubular lophophorate with brachiopod characters. *Scientific Reports*, 4:4682, doi:10.1038/srep04682.
- Zhao, F.-C., Hu, S.-X., Caron, J.-B., Zhu, M.-Y., Yin, Z.-J., and Lu, M. (2012). Spatial variation in the diversity and composition of the Lower Cambrian (Series 2, Stage 3) Chengjiang Biota, Southwest China. *Palaeogeography, Palaeoclimatology, Palaeoecology*, 346–347:54–65, doi:10.1016/j.palaeo.2012.05.021.
- Zhao, F.-C., Smith, M. R., Yin, Z.-J., Zeng, H., Li, G.-X., and Zhu, M.-Y. (2017). *Orthozanclus elongata* n. sp. and the significance of sclerite-covered taxa for early trochozoan evolution. *Scientific Reports*, 7(1):16232, doi:10.1038/s41598-017-16304-6.